



Systems-level analysis of *Escherichia coli* response to silver nanoparticles: The roles of anaerobic respiration in microbial resistance

Huamao Du^{a,1}, Tat-Ming Lo^a, Johnner Sitompul^b, Matthew Wook Chang^{a,*}

^a School of Chemical and Biomedical Engineering, Nanyang Technological University, Singapore 637459, Singapore

^b Department of Chemical Engineering, Faculty of Industrial Technology, Institute of Technology Bandung, Bandung 40132, Indonesia

ARTICLE INFO

Article history:

Received 12 June 2012

Available online 4 July 2012

Keywords:

Silver nanoparticles
Escherichia coli
Transcriptome analysis
Anaerobic metabolism
Antimicrobial resistance

ABSTRACT

Despite extensive use of silver nanoparticles for antimicrobial applications, cellular mechanisms underlying microbial response to silver nanoparticles remain to be further elucidated at the systems level. Here, we report systems-level response of *Escherichia coli* to silver nanoparticles using transcriptome-based biochemical and phenotype assays. Notably, we provided the evidence that anaerobic respiration is induced upon exposure to silver nanoparticles. Further we showed that anaerobic respiration-related regulators and enzymes play an important role in *E. coli* resistance to silver nanoparticles. In particular, our results suggest that *arcA* is essential for resistance against silver NPs and the deletion of *fnr*, *fdnH* and *narH* significantly increases the resistance. We envision that this study offers novel insights into modes of antimicrobial action of silver nanoparticles, and cellular mechanisms contributing to the development of microbial resistance to silver nanoparticles.

© 2012 Elsevier Inc. All rights reserved.

1. Introduction

Silver derivatives have been clinically used for antibacterial treatment since ancient times. In particular, silver nitrate and silver sulfadiazine ointments have been approved for application on wound dressings by U.S. Food and Drug Administration [1,2]. The application of silver derivatives for antibacterial treatment has recently drawn more attention because of the emergence of antibiotic-resistant pathogens [3]. Moreover, recent advances in nanotechnology have enabled the application of silver nanoparticles (NPs), which release silver ions, for dressings, textiles, implant apparatuses, and water filters [4].

Due to this proven efficacy of silver ions, prior studies have attempted to investigate their antimicrobial mechanisms. Silver ions reportedly increase Na⁺ permeability in *Bacillus* [5]; induce massive proton leakage from membrane in *Vibrio cholera* [6]; bind to enzymes through a sulfhydryl (thiol) group in amino acids [7]; uncouple a respiratory chain from oxidative phosphorylation [8]; simulate ATPase of mitochondria in rabbits; and cause a chromosome to lose its replication ability [9]. Further, the effects of silver NPs on cells include changes in cell size [10], shape [11], surface charge [12], organic matters, pH [13], and membrane composition [14]. A recent proteomic study of *Escherichia coli* response to silver

NPs suggests that envelope protein precursors are accumulated and proton motive force is dissipated after exposure to silver NPs [15]. Despite these prior studies, our understanding of bacterial response to silver NPs is still obscure at the systems level. Consequently, in this study, we studied a genome-wide response of *E. coli* K-12 to silver NPs using transcriptome-based biochemical and phenotype assays. For the first time, we provided the evidence that anaerobic respiration is significantly induced upon exposure to silver NPs, and anaerobic respiration-related regulators and enzymes play an important role in resistance to silver NPs. These results provide novel insights into antimicrobial mechanisms of silver NPs and cellular mechanisms contributing to the development of microbial resistance to silver NPs.

2. Material and Methods

2.1. Effects of silver NPs on growth and morphology

E. coli K12 BW25113 and its isogenic mutants (Table 1) were purchased from the Coli Genetic Stock Center. The cells were grown in a Luria–Bertani (LB) medium. A modified LB medium (LBm: 0.25% tryptone, 0.125% yeast extract, no sodium chloride, and pH 7.2) was used to re-suspend pellets before the cells were exposed to silver NPs (self-dispersed, 15 nm) dispersed in 0.1% BSA solution (pH 7.2). *E. coli* was grown to an optical density (at 600 nm; OD₆₀₀) of 0.3 and the cell pellet was suspended in LBm. This cell suspension was mixed with the equal volume of silver NP suspension and incubated at 37 °C and 100 rpm. The final

* Corresponding author. Fax: +65 6794 7553.

E-mail address: Matthewchang@ntu.edu.sg (M.W. Chang).

¹ Present address: College of Biotechnology, Southwest University, Chongqing 400715, China.

Table 1
E. coli strains used in this study.

Name	Description
7636	BW25113
JW4083-1	<i>ΔfumB748::kan</i>
JW2962	<i>ΔhybC767::kan</i>
JW2236	<i>ΔglpB722::kan</i>
JW1471	<i>ΔfdnH768::kan</i>
JW0886	<i>ΔpflB727::kan</i>
JW2194	<i>ΔnapA759::kan</i>
JW1216	<i>ΔnarH735::kan</i>
JW4364	<i>ΔarcA726::kan</i>
JW1328	<i>Δfnr771::kan</i>

Table 2
Primers used to clone *areA*, *fdnH*, and *narH* genes.

Name of primers	Sequences (5'-3')	Length (bp)
<i>arcA</i> -forward	GAAGAATTCATGCAGACCCGCACATTCT	717
<i>arcA</i> -reverse	GCAAAGCTTTTAATCTTCCAGATCACCGC	
<i>fdnH</i> -forward	CCCGAATTCATGGCTATGGAACGCAGGA	885
<i>fdnH</i> -reverse	GCCAAAGCTTTACTCATGATGATCCTCTCT	
<i>narH</i> -forward	CCCGAATTCATGAAAATTCGTTCAAGT	1539
<i>narH</i> -reverse	GAAAAGCTTTCATGGATGCGGTCCTGTTT	

concentrations of silver NPs in the mixture were 500, 250, 125, 62.5 and 31.25 μg/ml. Three biological replicates were used to generate a growth curve. For morphology analysis, *E. coli* cells exposed to 125 μg/ml of silver NPs suspension were examined using field emission scanning electron microscopy (FESEM, JFC-1600, 20 mA, 80 s) and transmission electron microscopy (TEM, Jeol 3010, 300 KV) as previously described [16,17].

2.2. Genome-wide transcription analysis

Total RNA was extracted from *E. coli* upon 5, 15, and 25 min exposure to 125 μg/ml of silver NPs. The *E. coli* Genome 2.0 array (Agilent) was used with two independent biological replicates, as

previously described [17]. The microarray data were analyzed using GeneSpring GX11 (Agilent).

2.3. ATP leakage, and Live/Dead staining assays

E. coli cells were harvested at OD 0.3 and suspended in the medium without sodium chloride. The cell suspension was subjected to ATP measurement upon 15 min exposure to silver NPs suspension (250 μg/ml) using BacTiter-Glo Reagent (Promega), and Luminex Reader (Promega). The extent of leakage of ATP was calculated as follows: leakage (%) = LUX (supernatant after treatment)/LUX (control cell). Three biological replicates were used, and the data were analyzed by ANOVA. For the Live/Dead assay, the treated and control cells were stained with Live/Dead mixed dyes at the room temperature for 15 min [18]. The images were acquired using a microscope (AX10, Zeiss), and merged using Image J program.

2.4. D-Lactate assay

E. coli was treated with 62.5 μg/ml silver NPs, and the controls were mixed with 0.1% BSA solution. The cells were collected after 1 and 2 h treatment, and centrifuged at 1000 rpm for 5 min at 4 °C. The supernatants were filtrated through 3 KD Milicon Ultrfilter (Millipore). D-Lactate Assay Kit K667 (BioVision) was used following the manufacture's protocol. The background was subtracted from the readings of all samples, and the concentrations were calculated according to the standard curve. The assay was carried out with three biological replicates.

2.5. Survival of isogenic mutants

To understand the roles of genes expressed in the course of silver NPs treatment, a survival assay was performed after 15 min and 24 h treatments. The 15 min treatment was conducted with planktonic cells, while the 24 h treatment was conducted using silver NPs on agar plates because silver NPs tend to aggregate in aqueous solution after long incubation. For the 15 min treatment, *E. coli* and other eight isogenic mutants were grown in LB to OD of 0.3, diluted by 10-fold, and then mixed with silver NPs (final concentration: 125 μg/ml) at 37 °C with shaking at 100 rpm for

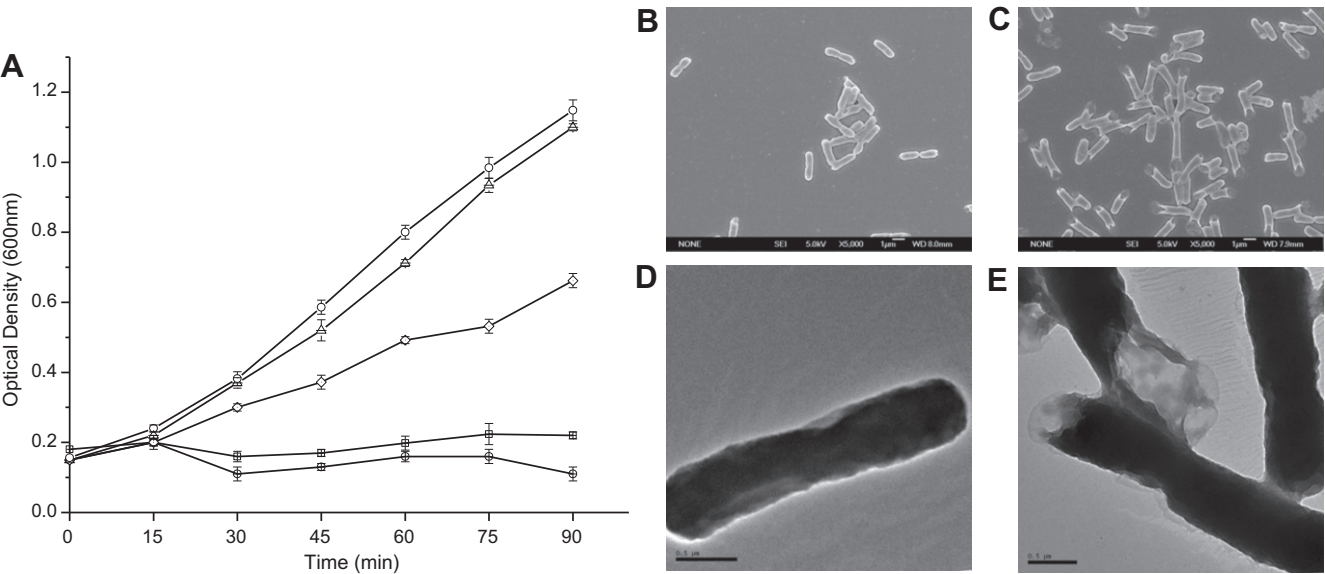


Fig. 1. (A) Growth curve of *E. coli* K-12 BW25113 during exposure to silver NPs. The results represent the averages of three biological replicates with standard deviations. Morphological changes of *E. coli* treated with silver NPs under aerobic condition are shown as follows. FESEM images of the *E. coli* cells with (B) and without (C) the treatment, respectively. TEM images of the *E. coli* cells with (D) and without (E) the treatment, respectively.

Table 3

Anaerobic respiration-related genes regulated by silver NPs.

Gene	Locus tag	Gene Product	Fold change (FC)	Regulons
narG	b1224	nitrate reductase 1, alpha subunit	94.64	FNR(+), IFN(+), NarL(+), PstA(+), Fis(–),
narH	b1225	nitrate reductase 1, beta subunit	165.28	
narJ	b1226	nitrate reductase 1, delta subunit, assembly function	53.42	
narI	b1227	nitrate reductase 1, cytochrome b	88.29	
nirB	b3365	nitrite reductase	102.13	
nirD	b3366	nitrite reductase	106.89	NarL(+), NarP(+), FNR(+), CRP(–), Fis(–), FruR(–), HNS(–), IHF(±)
nrfA	b4070	periplasmic cytochrome c	47.43	NarP(+), FlhDC(+), FNR(+), IHF(+), NsrR(–), Fis(–), NarL(±),
nrfB	b4071	formate-dependent nitrite reductase	116.68	
nrfC	b4072	formate-dependent nitrite reductase; Fe-S centers	102.59	
nrfD	b4073	formate-dependent nitrate reductase complex	36.87	
nrfE	b4074	formate-dependent nitrite reductase	12.57	
nrfF	b4075	part of formate-dependent nitrite reductase complex	4.73	NarL(+), FNR(±), NarP(–),
nrfG	b4076	part of formate-dependent nitrite reductase complex	19.76	
fdnG	b1474	formate dehydrogenase-N, alpha subunit	94.78	
fdnH	b1475	formate dehydrogenase-N, iron-sulfur beta subunit	79.37	
fdnI	b1476	formate dehydrogenase-N	32.46	
dmsA	b0894	anaerobic dimethyl sulfoxide reductase subunit A	52.13	FNR(+), Fis(–), IHF(–), ModE(–), NarL(–)
dmsB	b0895	anaerobic dimethyl sulfoxide reductase subunit B	58.26	
dmsC	b0896	anaerobic dimethyl sulfoxide reductase subunit C	27.27	
napC	b2202	cytochrome c-type protein	29.80	
napB	b2203	cytochrome c-type protein	28.67	
napH	b2204	ferredoxin-type protein: electron transfer	43.50	FlhDC(+), FNR(+), ModE(+), IscR(–), NarL(–), NarP(±),
napG	b2205	ferredoxin-type protein: electron transfer	43.85	
napA	b2206	probable nitrate reductase 3	49.77	
napD	b2207	hypothetical protein	14.70	
glpA	b2241	sn-glycerol-3-phosphate dehydrogenase	25.07	
glpB	b2242	sn-glycerol-3-phosphate dehydrogenase	41.34	CRP(+), Fis(+), FlhDC(+), FNR(+), ArcA(–), GlpR(–)
glpC	b2243	sn-glycerol-3-phosphate dehydrogenase	36.69	
glpR	b3423	repressor of the glp operon	–2.45	
pflA	b0902	pyruvate formate lyase activating enzyme 1	2.94	
pflB	b0903	formate acetyltransferase 1	5.97	
hyaA	b0972	hydrogenase-1 small subunit	4.7	IHF(+), ArcA(+), FNR(+), CRP(+), Fis(–), NarL(–) AppY(+), ArcA(+), Fis(–), IscR(–), NarL(–), NarP(–),
hyaE	b0976	processing of HyaA and HyaB proteins	2.48	
nikD	b3479	ATP-binding protein of nickel transport system	35.92	
nikE	b3480	ATP-binding protein of nickel transport system	41.59	
fumB	b4122	fumarate hydratase Class I	4.58	
hybG	b2990	hydrogenase-2 operon protein: may effect maturation of large subunit of hydrogenase-2	5.4	FNR(+), ArcA(–), CRP(+), Fur(+), DcuR(+), NarL(–), Fis(–) NarL(–), ArcA(–),
hybF	b2991	may modulate levels of hydrogenase-2	4.06	
hybD	b2993	probable processing element for hydrogenase-2	4.17	
hybC	b2994	probable large subunit, hydrogenase-2	8.04	
hybB	b2995	probable cytochrome Ni/Fe component of hydrogenase-2	11.44	
hybO	b2997	putative hydrogenase subunit	13.64	NT NT ArcA(+), CRP(+), Fis(+), PdhR(–), FNR(±)
pykA	b1854	pyruvate kinase II	5.56	
yjyW	b4379	putative activating enzyme	41.11	
yfiD	b2579	putative formate acetyltransferase	3.53	
menC	b2261	o-succinylbenzoyl-CoA synthase	2.16	
menB	b2262	dihydroxynaphthoic acid synthetase	2.36	NT FhlA(+), FNR(+), IHF(+), NsrR(–),
hypF	b2712	transcriptional regulatory protein	5.45	
hypC	b2728	pleiotrophic effects on 3 hydrogenase isozymes	20.44	
hypD	b2729	pleiotrophic effects on 3 hydrogenase isozymes	18.62	
hypE	b2730	plays structural role in maturation of all 3 hydrogenases	13.48	
acnA	b1276	aconitate hydratase 1	–2.16	FNR(–), AcrA(–), FruR(+), CRP(+), FNR(–), IHF(–), NsrR(–), PdhR(–), ArcA(+), Fis(±) FhlA(+), FlhDC(+), FhlA(+),
ndh	b1109	respiratory NADH dehydrogenase	–2.43	
hydN	b2713	involved in electron transport from formate to hydrogen, Fe-S centers	–2.48	

15 min. Three biological replicates were used for each strain. The cells before and after the treatment were counted on LB agar plates. Survival (%) = [(mean CFU/ml of treated sample)/(mean CFU/ml of control sample)] × 100. For the 24 h treatment, a series of agar plates containing the following concentrations of silver NPs were used: 40, 60, 80, and 100 µg/ml. Agar plates containing 500 µg/ml silver NPs were used to examine survival under anaerobic condition. The cells were dropped onto the silver NPs agar plates and the plate sets were transferred to aerobic and anaerobic incubators, and incubated for 24 h at 37 °C.

2.6. Sensitivity of complement strains to silver NPs

The recombinant plasmids, pBAD30-arcA, pBAD30-fdnH, and pBAD30-narH were transformed into JW4364-1, JW1216-2 and JW1471-1, respectively (Table 2). To construct negative controls, pBAD30 was transformed into three mutant strains and the wild type strain. All complements and controls were grown in LB with ampicillin (100 µg/ml) with arabinose (final concentration: 0.2%) as an inducer [19]. The sensitivity was measured using agar plates containing a range of concentrations of silver NPs (60–100 µg/ml).

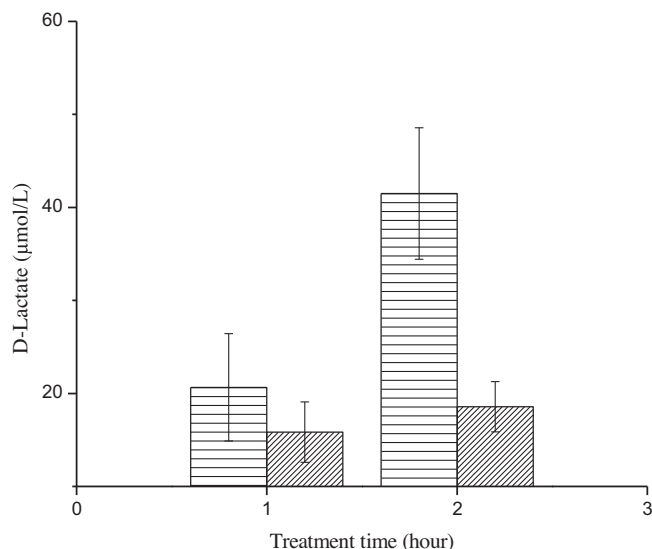


Fig. 2. The amount of D-lactate produced with (horizontal stripes) and without (diagonal stripes) silver NPs.

3. Results and discussion

3.1. Effects of silver nanoparticles on growth and morphology of *E. coli*

To determine the antimicrobial efficacy of silver NPs, *E. coli* was exposed to silver NPs at a range of concentrations. Fig. 1A shows that the growth of *E. coli* was significantly inhibited at 62.5 μg/ml and no growth was observed at 125 and 250 μg/ml, whereas *E. coli* seemed to grow normally at 31.25 μg/ml. To examine morphological changes by silver NPs, *E. coli* cells were observed under field emission scanning electron microscope (FESEM) and transmission electron microscope (TEM) upon exposure to silver NPs. The FESEM analysis indicates membrane disruption and lysis by silver NPs, while the control cells exhibited clear structure, and the cell surface remained intact (Fig. 1B and C). Intriguingly, a number of *E. coli* cells exposed to silver NPs had a relatively long shape, compared to the control cells, which may imply cell division inhibition by silver NPs. The TEM analysis shows that silver NPs

caused severe damage to the cell membrane, indicated by the collapsed cell structure (Fig. 1D and E).

3.2. Transcriptome analysis of *E. coli* response to silver NPs

To investigate cellular mechanisms associated with antimicrobial effects of silver NPs, we conducted genome-wide transcription analysis upon 5, 15, and 25 min exposure to silver NPs. Briefly, the transcriptome data suggest that (i) 9 genes were up-regulated after 5 min treatment; (ii) 108 genes were differently expressed after 15 min, while 72 genes were up-regulated; and (iii) 458 genes were differently expressed after 25 min, with 260 up-regulated genes. Intriguingly, the transcriptome response of *E. coli* to silver NPs involves the up-regulation of copper/silver resistance genes, including *cusBCF*, *copA* and *cueO* (*cusB*: 128-fold, *cusF*: 80-fold, *cusC*: 79.5-fold, *cusA*: 39-fold, *copA*: 70-fold, and *cueO*: 20.5-fold at 15 min). These genes remained up-regulated at 25 min but the extent of the upregulation was decreased to 7–20-fold. Another notable observation was that many anaerobic respiration-related reductases were up-regulated at 15 and 25 min, whereas aerobic respiration-related oxidases, such as *ndh*, *mgo* [20] and *cyoBCE* operon, were down-regulated. Further, the 35 most up-regulated genes are all involved in anaerobic respiration, including the *nar* regulons, and the *nir*, *nap*, *nrf*, *fdn*, *dms*, and *glp* operons (Table 3).

3.3. Effects of silver NPs on respiration mechanisms

Since the genome-wide transcription analysis indicated the induction of anaerobic respiration-related genes, we hypothesized that anaerobic respiration might be stimulated upon exposure to silver NPs. To test this hypothesis, we measured the amount of D-lactate, a major product of anaerobic metabolism. Fig. 2 shows that the concentration of D-lactate produced was higher when the cells were exposed to silver NPs, and the difference became more evident upon 2 h exposure. This result along with the repression of genes of the Krebs cycle provides the evidence that anaerobic respiration is stimulated during exposure to silver NPs.

3.4. Effects of oxygen availability on the antimicrobial activity of silver NPs

The results above suggest that anaerobic respiration was stimulated upon exposure to silver NPs. Therefore, to study whether

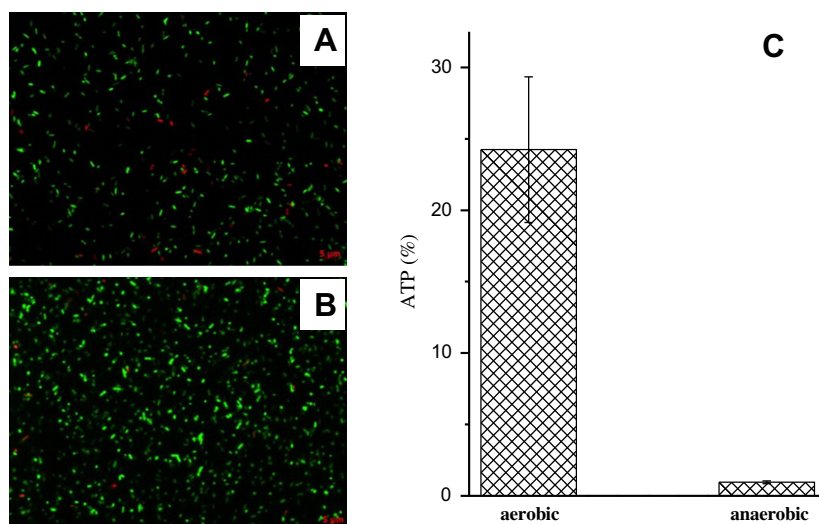


Fig. 3. Comparison of membrane permeability of *E. coli* treated with silver NPs under aerobic (A) and anaerobic condition (B) using the Live/Dead dyes, and ATP leakage assay (C). The data represent the averages of three biological replicates with standard deviations.

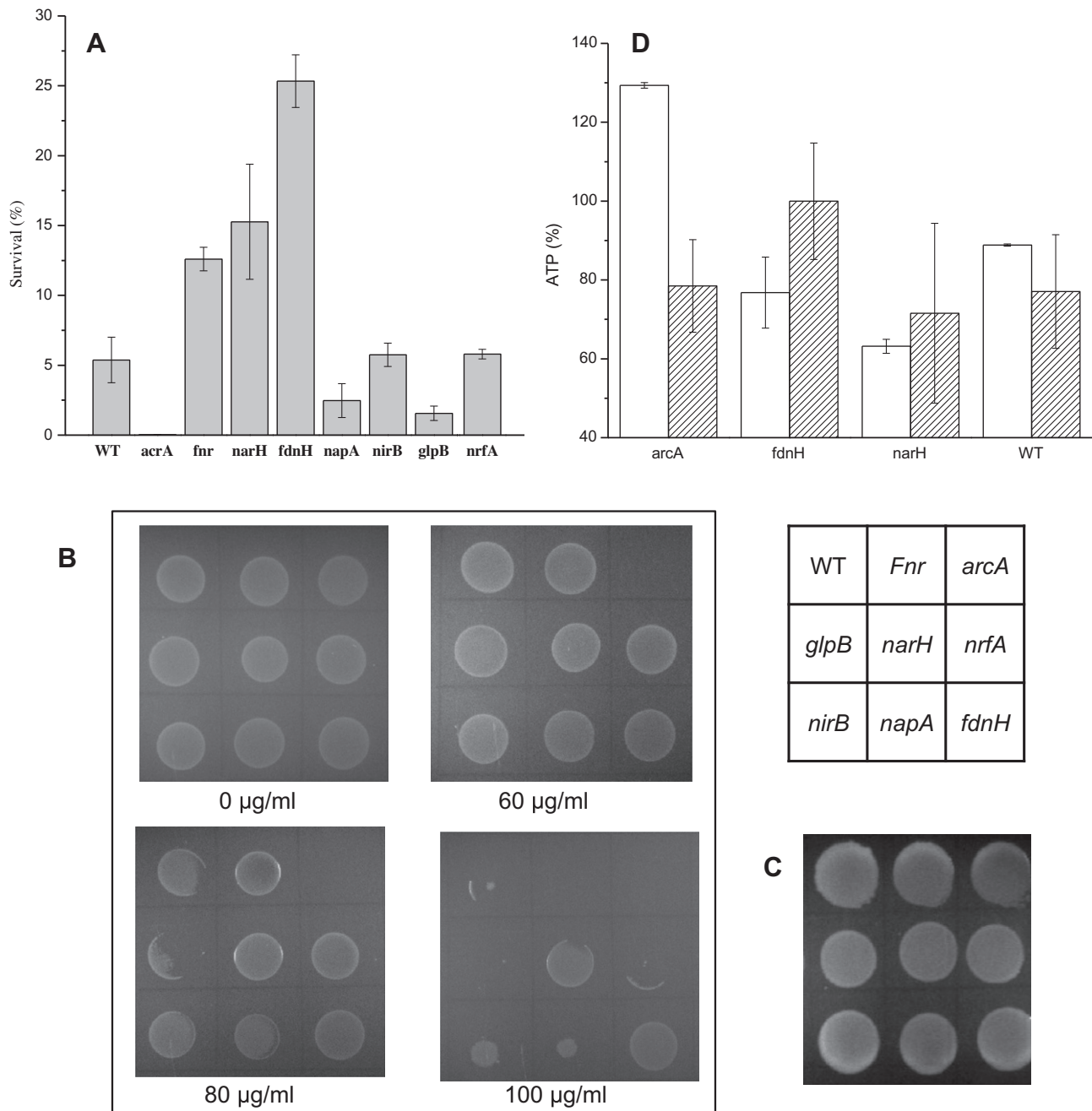


Fig. 4. Survival rates of *E. coli* isogenic mutants lacking anaerobic respiration-related genes *fnr*, *arcA*, *glpB*, *narH*, *nrfA*, *nirB*, *napA*, and *fdnH* upon 15 min (A) and 24 h (B) exposure to silver NPs under aerobic condition. The rectangular box with the names of the aforementioned genes shows the location of the corresponding mutants on agar plates. The data represent the averages of three biological replicates with standard deviations. (C) Survival rates of the cells treated with 500 µg/ml silver NPs for 24 h under anaerobic condition. (D) Measurement of ATP leakage of *E. coli* cells complemented without (white bar) and with (striped bar) the expression of the specified genes.

oxygen availability is also related to the antimicrobial activity of silver NPs, we examined membrane damage by silver NPs under both aerobic and anaerobic condition, using Live/Dead cell viability and ATP leakage assays. Fig. 3A and B shows that more *E. coli* cells were stained with the propidium iodide (red) dye, which penetrates damaged membrane. Fig. 3C shows that the amount of ATP released from the cells was 10 times higher under aerobic conditions than under anaerobic conditions, which indicates that membrane damage by silver NPs was much more significant under aerobic conditions. These results suggest that membrane disruption induced by silver NPs is an oxygen-dependent process, in line with a previous study reporting that membrane damage by silver NPs is likely due to lipid peroxidation by reactive oxygen species [21].

3.5. ArcA and Fnr regulators are associated with silver NPs resistance

Based on the abovementioned results, to determine the roles of transcription regulators associated with intracellular oxygen availability, we have examined the survival rate of *fnr* and *arcA* knock-out mutants upon 15 min and 24 h treatment with silver NPs under aerobic condition. FNR and ArcAB are essential regulators that control metabolism according to oxygen availability. In Fig. 4A, the *fnr* and *arcA* knock-out mutants shows higher and lower survival rates, respectively, than the wild-type cells after 15 min (Fig. 4A) and 24 h (Fig. 4B) treatment with silver NPs. This result suggests that ArcA and FNR are associated with cellular resistance to silver NPs in *E. coli*. Note that those mutants showed resistance

up to 500 µg/ml under anaerobic condition (Fig. 4C). Further, to validate the essentiality of *ArcA* in silver NP resistance under aerobic condition, we expressed the *arcA* gene in the *arcA* knock-out mutant using recombinant plasmid pBAD30-*arcA*. Fig. 4D shows that ATP leakage became much lower when *arcA* was complementarily expressed in the *arcA* mutant, implying that *ArcA* is essential for cellular resistance to silver NPs under aerobic condition.

3.6. Redox enzymes associated with silver NP resistance

Because oxygen availability is closely linked to intracellular redox reactions, we have examined the survival rates of the mutants lacking six redox and anaerobic respiration related enzyme genes, *glpB*, *nrfA*, *nirB*, *napA*, *fdnH* and *narH*, upon 15 min and 24 h treatment with silver NPs under aerobic condition. Those six genes also showed significant changes in transcription level according to the transcriptome analysis. Fig. 4A shows that the survival rates of the *narH* and *fdnH* mutants were much higher than the wild-type cells, which was in line with the resistance levels obtained from the 24 h treatment, where the *fdnH* and *narH* mutants could grow even against 100 µg/ml silver NPs (Fig. 4B). Note that those mutants showed resistance up to 500 µg/ml under anaerobic condition (Fig. 4C). Fig. 4 shows that ATP leakage was increased upon complementation of the *fdnH* and *narH* mutants by the expression of *fdnH* and *narH*, respectively, which suggests that the knock-out of *fdnH* and *narH* led to increased resistance to silver NPs under aerobic condition.

In conclusion, for the first time, we provided the evidence that anaerobic respiration was simulated upon exposure to silver NPs using transcriptome-based biochemical and phenotypic analyses. In particular, we showed that among anaerobic respiration related genes, the deletion of *fnr*, *fdnH* and *narH* significantly increased cellular resistance against silver NPs, whereas the deletion of *arcA*, *napA* and *glpB* decreased the resistance. Our results offer novel insights into modes of antimicrobial action of silver NPs, and cellular mechanisms contributing to the development of microbial resistance to silver nanoparticles.

Acknowledgments

This research was funded by Environment and Water Industry Programme Office of Singapore (0802-IRIS-12) and the National Research Foundation of Singapore (NRF-CRP5-2009-03).

References

- [1] H.J. Klasen, Historical review of the use of silver in the treatment of burns. I. Early uses, *Burns* 26 (2000) 117–130.
- [2] H.J. Klasen, A historical review of the use of silver in the treatment of burns. II. Renewed interest for silver, *Burns* 26 (2000) 131–138.

- [3] H.H. Lara, N.V. Ayala-Nunez, L.D.I. Turrent, C.R. Padilla, Bactericidal effect of silver nanoparticles against multidrug-resistant bacteria, *World J. Microbiol. Biotechnol.* 26 (2010) 615–621.
- [4] F. Furno, K.S. Morley, B. Wong, B.L. Sharp, P.L. Arnold, S.M. Howdle, R. Bayston, P.D. Brown, P.D. Winship, H.J. Reid, Silver nanoparticles and polymeric medical devices: a new approach to prevention of infection?, *J. Antimicrob. Chemother.* 54 (2004) 1019–1024.
- [5] A.L. Semeykina, V.P. Skulachev, Submicromolar Ag⁺ increases passive Na⁺ permeability and inhibits the respiration-supported formation of Na⁺ gradient in bacillus FTU vesicles, *FEBS Lett.* 269 (1990) 69–72.
- [6] P. Dibrov, J. Dzioba, K.K. Gosink, C.C. Hase, Chemiosmotic Mechanism of Antimicrobial Activity of Ag⁺ in *Vibrio cholerae*, *Antimicrob. Agents Chemother.* 46 (2002) 2668–2670.
- [7] O. Gordon, T. Vig Slenters, P.S. Brunetto, A.E. Villaruz, D.E. Sturdevant, M. Otto, R. Landmann, K.M. Fromm, Silver Coordination Polymers for Prevention of Implant Infection: Thiol Interaction, Impact on Respiratory Chain Enzymes, and Hydroxyl Radical Induction, *Antimicrob. Agents Chemother.* 54 (2010) 4208–4218.
- [8] K.B. Holt, A.J. Bard, Interaction of silver(I) ions with the respiratory chain of *Escherichia coli*: An electrochemical and scanning electrochemical microscopy study of the antimicrobial mechanism of micromolar Ag, *Biochemistry* 44 (2005) 13214–13223.
- [9] Q.L. Feng, J. Wu, G.Q. Chen, F.Z. Cui, T.N. Kim, J.O. Kim, A mechanistic study of the antibacterial effect of silver ions on *Escherichia coli* and *Staphylococcus aureus*, *J. Biomed. Mater. Res.* 52 (2000) 662–668.
- [10] J.R. Morones, J.L. Elechiguerra, A. Camacho, K. Holt, J.B. Kouri, J.T. Ramirez, M.J. Yacaman, The bactericidal effect of silver nanoparticles, *Nano Technol.* 16 (2005) 2346–2353.
- [11] S. Pal, Y.K. Tak, J.M. Song, Does the Antibacterial Activity of Silver Nanoparticles Depend on the Shape of the Nanoparticle? A Study of the Gram-Negative Bacterium *Escherichia coli*, *Appl. Environ. Microbiol.* 73 (2007) 1712–1720.
- [12] C.-N. Lok, C.-M. Ho, R. Chen, Q.-Y. He, W.-Y. Yu, H. Sun, P.K.-H. Tam, J.-F. Chiu, C.-M. Che, Silver nanoparticles: partial oxidation and antibacterial activities, *J. Biol. Inorg. Chem.* 12 (2007) 527–534.
- [13] J. Fabrega, S.R. Fawcett, J.C. Renshaw, J.R. Lead, Silver Nanoparticle Impact on Bacterial Growth: Effect of pH, Concentration, and Organic Matter, *Environ. Sci. Technol.* 43 (2009) 7285–7290.
- [14] S. Shrivastava, T. Bera, A. Roy, G. Singh, P. Ramachandrarao, D. Dash, Characterization of enhanced antibacterial effects of novel silver nanoparticles, *Nanotechnology* 18 (2007).
- [15] C.N. Lok, C.M. Ho, R. Chen, Q.Y. He, W.Y. Yu, H.Z. Sun, P.K.H. Tam, J.F. Chiu, C.M. Che, Proteomic analysis of the mode of antibacterial action of silver nanoparticles, *J. Proteome Res.* 5 (2006) 916–924.
- [16] H. Ling, A. Kang, M.H. Tan, X. Qi, M.W. Chang, The absence of the *luxS* gene increases swimming motility and flagella synthesis in *Escherichia coli* K12, *Biochem. Biophys. Res. Commun.* 401 (2010) 521–526.
- [17] A. Kang, M.W. Chang, Identification and reconstitution of genetic regulatory networks for improved microbial tolerance to isooctane, *Mol. Biosyst.* 8 (2012) 1350–1358.
- [18] N. Saeidi, C.K. Wong, T.M. Lo, H.X. Nguyen, H. Ling, S.S. Leong, C.L. Poh, M.W. Chang, Engineering microbes to sense and eradicate *Pseudomonas aeruginosa*, a human pathogen, *Mol. Sys. Biol.* 7 (2011) 521.
- [19] D.K. Tay, G. Rajagopalan, X. Li, Y. Chen, L.H. Lua, S.S. Leong, A new bioproduction route for a novel antimicrobial peptide, *Biotechnol. Bioeng.* 108 (2011) 572–581.
- [20] M.E. van der Rest, C. Frank, D. Molenaar, Functions of the membrane-associated and cytoplasmic malate dehydrogenases in the citric acid cycle of *Escherichia coli*, *J. Bacteriol.* 182 (2000) 6892–6899.
- [21] C. Carlson, S.M. Hussain, A.M. Schrand, L.K. Braydich-Stolle, K.L. Hess, R.L. Jones, J.J. Schlager, Unique cellular interaction of silver nanoparticles: size-dependent generation of reactive oxygen species, *J. Phys. Chem. B* 112 (2008) 13608–13619.